Experimental Characterization of Hot-Electron Emission and Shock Dynamics in the Context of the Shock-Ignition Approach to Inertial Confinement Fusion

A. Tentori,[1] A. Colaïtis,[1] W. Theobald,[2,3] A. Casner,[1] D. Raffestin,[1] A. Ruocco,[1,4] J. Trela,[1] E. Le Bel,[1] K. S. Anderson,[2] M. S. Wei,[2] B. J. Henderson,[2] J. L. Peebles,[2] R. Scott,[4] S. Baton,[5] S. A. Pikuz,[6] R. Betti,[2,3,7] M. Khan,[8] N. Woolsey,[8] and D. Batani[1]

[1]Centre Lasers Intenses et Applications, CELIA, Université Bordeaux, France
[2]Laboratory for Laser Energetics, University of Rochester
[3]Department of Mechanical Engineering, University of Rochester
[4]Central Laser Facility, STFC Rutherford Appleton Laboratory, United Kingdom
[5]Laboratoire pour l'Utilisation des Lasers Intenses, CNRS-Ecole Polytechnique-CEA-Sorbonne Universités, France
[6]Joint Institute for High Temperatures of Russian Academy of Sciences, Russia
[7]Department of Physics and Astronomy, University of Rochester
[8]York Plasma Institute, Department of Physics, University of York, United Kingdom

Shock ignition (SI) is an alternative approach to direct-drive inertial confinement fusion based on the separation of the compression and the ignition phases.[1,2] The high laser intensity required in the ignition phase exceeds the thresholds for the generation of laser–plasma instabilities,[3] generating a large amount of suprathermal electrons. Depending on their characteristics these electrons could preheat the hot spot with detrimental effects for the SI scheme, or assist in generating a strong shock.[4]

Here we report on a planar target experiment conducted on the OMEGA EP Laser System aimed at characterizing the hot-electron source and the shock dynamics using laser parameters relevant for SI. A UV ($\lambda = 351$-nm) laser beam was tightly focused on planar multilayer targets, providing a nominal vacuum laser intensity of $\sim 10^{16}$ W/cm^2 with a pulse duration of ~1 ns. The laser energy delivered was ~1250 J. The planar targets consisted of 500-μm-diam disks with two layers (175 or 250 μm of CH, or 20 or 10 μm of Cu). These were mounted on a 50-μm-thick CH slab intended to inhibit hot-electron recirculation. The UV interaction laser impinged on the front of the CH ablator, generating a strong shock and large amounts of hot electrons. The shock propagation was monitored using x-ray time-resolved radiographs; the x-ray source was created by focusing a second laser beam (4×10^{14} W/cm^2, 3-ns pulse duration) on a V foil. This scheme allows production of copious amounts of V K_α x rays that pass through the target; the x rays are then detected by a four-strip x-ray framing camera (XRFC).[5] The camera was equipped with a 4×4 array of 20-μm-diam pinholes, capturing 16, 2-D images of the shock front at different times with 6× magnification (Fig. 1).

Hot electrons were characterized using separate x-ray spectrometers. The hot-electron–produced bremsstrahlung radiation was diagnosed by two time-integrating hard x-ray spectrometers (BMXS's).[6] The instruments are composed of a stack of 15 imaging plates alternated by filters of different metals. The total yield of Cu K_α was measured by an absolutely calibrated zinc von Hamos x-ray spectrometer (ZnVH).[7]

The post-processing of the spectrometers relies on cold Monte Carlo methods [Geant4 (Ref. 8)] in which the electron transport and the x-ray generation on the diagnostics are simulated. In particular, electrons are assumed to be energetically described by a 2-D Maxwellian function:

$$f_e(E) = \frac{N_e}{T_h} e^{-E/T_h}.$$

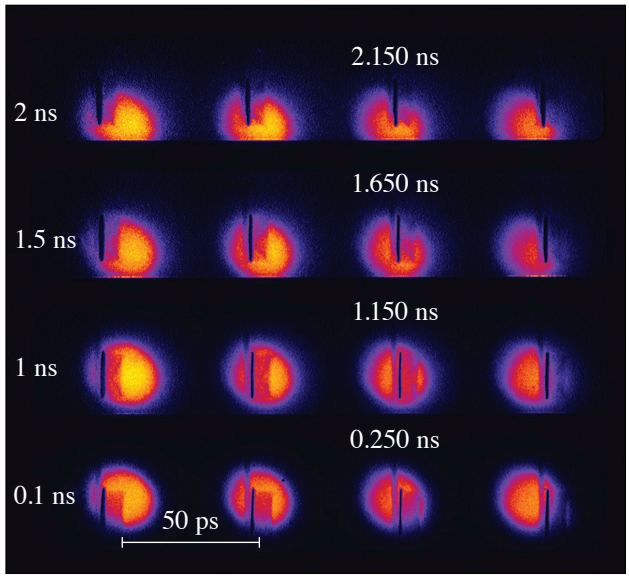

Figure 1
Array of 2-D radiographs captured at various times by the XRFC for shot 28407. Line spacing between each image is 50 ps.

The parameters N_e and T_h that reproduce both the experimental bremsstahlung spectrum and the K_α signal detected by the BMXS's and the ZnVH are calculated. A large uncertainty on the values of N_e and T_h arises because of the disagreement among the results from different shots and because of the systematic disagreement between the two diagnostics. A disagreement of ~25% is also noted in the simulations of the K_α signal using two different libraries of Geant4.[9,10] As such, T_h ranges from 20 keV up to 50 keV and N_e from 4×10^{16} down to 5×10^{15}. It is therefore necessary to consider the hydrodynamic evolution of the target to reduce these large ambiguities. In particular, we considered three representative hot-electron distribution functions to use as input in the hydrodynamic simulations to determine which *combination* of laser to hot-electron energy conversion efficiency η and average temperature T_h better reproduces the experimental behavior observed in the radiographs. The three representative $f_e(E)$ are reported in Table I.

Table I: Parameters of Maxwellian functions $f_e(E)$ obtained from post-processing the BMXS and ZnVH diagnostic data for shot 28407, used as input in *CHIC*.

$f_e(E)$			
	T_h (keV)	N_e (10^{16})	η (%)
$f_{e1}(E)$	26	3.4	11
$f_{e2}(E)$	35	1.4	6
$f_{e3}(E)$	45	0.5	3

The radiation-hydrodynamic simulations were performed with the code *CHIC*,[11] in which a model of hot-electron transport is included.[12] The shock position and the copper plate expansion are the figures of merit used to characterize the hot-electron source. Different intensities and kinetic energies of the hot-electron beam will strongly affect the variation in time of these two quantities. The simulations showed that an electron beam described by $f_{e1}(E)$ and $f_{e2}(E)$ allows reproduction of the experimental behavior.

According to the simulations hot electrons with these characteristic values of η and T_h increase the shock pressure up to 150 Mbar, 25 Mbar more than the value predicted by simulations without the hot-electron beam included. The effects of such an electron distribution function on a typical SI imploded target[13] were evaluated using a simple ideal-gas equation-of-state model. An increase of the shell adiabat was calculated using the high conversion efficiency found in the experiment, which could represent an issue for the SI scheme.

This material is based upon work supported by the Department of Energy National Nuclear Security Administration under Award Number DE-NA0003856, the University of Rochester, and the New York State Energy Research and Development Authority.

1. V. A. Shcherbakov, Sov. J. Plasma Phys. **9**, 240 (1983).
2. R. Betti *et al*., Phys. Rev. Lett. **98**, 155001 (2007).
3. W. L. Kruer, *The Physics of Laser Plasma Interactions*, edited by D. Pines, 1st ed. (CRC Press, Boca Raton, FL, 2003).
4. S. Gus'kov *et al*., Phys. Rev. Lett. **109**, 255004 (2012).
5. D. K. Bradley *et al*., Rev. Sci. Instrum. **63**, 4813 (1992).
6. C. D. Chen *et al*., Rev. Sci. Instrum. **79**, 10E305 (2008).
7. L. C. Jarrott *et al*., Rev. Sci. Instrum. **88**, 043110 (2017).
8. S. Agostinelli *et al*., Nucl. Instrum. Methods Phys. Res. A **506**, 250 (2003).
9. F. Salvat, *PENELOPE 2018: A Code System for Monte Carlo Simulation of Electron and Photon Transport*, Nuclear Energy Agency (OECD Publishing, Paris, France, 2019).
10. S. T. Perkins *et al*., Lawrence Livermore National Laboratory, Livermore, CA, Report UCRL-50400 (1991).
11. J. Breil, S. Galera, and P.-H. Maire, Comput. Fluids **46**, 161 (2011).
12. A. Colaïtis *et al*., Phys. Rev. E **92**, 041101(R) (2015).
13. A. Colaïtis *et al*., Phys. Plasmas **23**, 072703 (2016).